

## Exciting circular TE<sub>mn</sub> modes at low terahertz region

T. H. Chang,<sup>a)</sup> C. H. Li, C. N. Wu, and C. F. Yu

Department of Physics, National Tsing Hua University, Hsinchu 30013, Taiwan

(Received 17 July 2008; accepted 28 August 2008; published online 18 September 2008)

This work proposes an approach to generate circular TE<sub>mn</sub> modes at low terahertz region through sidewall couplings. With proper arrangement of the couplings on the circumference of the waveguide, they then jointly excite the desired mode. A model is developed to calculate the coupling strength and to analyze the mode purity. Accordingly, three mode converters TE<sub>21</sub>, TE<sub>01</sub>, and TE<sub>41</sub>, were designed, built, and tested at *W*-band. Back-to-back transmission measurements exhibit excellent agreement with the results of simulations. The measured optimal transmissions are 91%, 95%, and 89% with 3 dB bandwidths of 18.3, 24.0, and 20.2 GHz, respectively. © 2008 American Institute of Physics. [DOI: 10.1063/1.2987486]

Research in the terahertz region has drawn much attention in recent years. The low-power and noncoherent radiation sources have created numerous applications, while the development of the high-power and coherent radiations is still slow-paced because of the severe lack of radiation sources as well as devices, such as mode converters. The gyrotrons are ideal radiation sources, based on the electron cyclotron maser mechanism.<sup>1</sup> A mode converter is needed to launch the desired wave into the interaction region (e.g. traveling-wave amplifier) or to extract a wave power from the interaction region (e.g. backward-wave oscillator). A poor mode converter, however, excites unwanted modes resulting in severe mode-competition problem and significantly hinders the progress of high-power terahertz gyrotrons.

Excitation of a circular TE<sub>mn</sub> mode is classified into two categories, according to the coupling methods involved. One is in-line coupling<sup>2-6</sup> and the other is sidewall coupling.<sup>7-12</sup> The latter generally uses a smooth waveguide with coupling holes on the sidewall. If the transition length is long, multiple modes could be excited during the converting process, resulting in severe mode competition. To avoid such drawbacks, the sidewall couplings around the circumference of the circular waveguide are generally employed. Such couplings can be achieved by a coaxial cavity<sup>7</sup> or by a *Y*-type power divider,<sup>8,9</sup> for example. The coaxial cavity, which connects a rectangular waveguide and a circular waveguide, has been adopted and shown very effective but limited in bandwidth. Recently, the *Y*-type power divider, which partitions a wave into several proportional signals and then injects to the circular waveguide, was used and shown excellent performance at *Ka*-band.<sup>8,9</sup> However, the working principle was not clearly explained.

This work presents a generic approach to excite a pure circular TE<sub>mn</sub> mode through sidewall couplings with the emphasis on the coupling mechanism. The couplings inducing the electric or magnetic dipoles and jointly synthesizing the desired mode will be analyzed in details. Based on this methodology, three mode converters will be designed and fabricated. These high-performance converters are demonstrated at *W*-band. They are suitable for gyrotron amplifier/oscillator applications.

*Mode synthesizing.* Table I summarizes the main parameters for the three mode converters TE<sub>21</sub>, TE<sub>01</sub>, and TE<sub>41</sub>. To excite the TE<sub>21</sub> mode, only three parasitic (unwanted) modes, the TE<sub>11,A</sub>, TE<sub>11,B</sub>, and TM<sub>01</sub> modes, need to be considered, where the subindices *A* and *B* denote the degenerate modes. However, to generate the TE<sub>41</sub> mode, we have to deal with as many as fourteen parasitic modes. This, of course, is very difficult.

Figure 1 illustrates the geometry of a single sidewall coupling under study. A rectangular waveguide mode (normally the TE<sub>10</sub> mode) is converted into the desired circular waveguide mode (TE<sub>mn</sub> mode) through sidewall couplings. Such coupling structure excites the magnetic dipole moment ( $\bar{P}_m$ ) only. To demonstrate how this principle works, the TE<sub>41</sub> mode is chosen for two reasons—it is very difficult and never reported before, and it is the key device for the fourth cyclotron harmonic gyrotrons. The field pattern of the TE<sub>41</sub> mode suggests a quad-feed arrangement of the input signals. Proper couplings effectively suppress the parasitic modes. In the following discussion, the waveguide is assumed to be parallel to *z* axis for simplicity. So the equivalent magnetic polarization current is

$$\bar{M} = j\omega\mu_0\bar{P}_m = -j\omega\mu_0\alpha_m H_z \delta(\rho - \rho_0) \delta(z - z_0) \hat{z} \cdot \left[ \delta(\phi - 0) + \delta\left(\phi - \frac{\pi}{2}\right) + \delta(\phi - \pi) + \delta\left(\phi - \frac{3\pi}{2}\right) \right], \quad (1)$$

where the wave is assumed to be sinusoidal time-dependent

TABLE I. The design parameters and its corresponding parasitic modes for TE<sub>21</sub>, TE<sub>01</sub>, and TE<sub>41</sub> modes.

Desired mode	TE <sub>21</sub>	TE <sub>01</sub>	TE <sub>41</sub>
Couplings	Dual feed	Quad feed	Quad feed
Waveguide radius	1.74 mm	2.15 mm	3.00 mm
	TE <sub>11,A</sub> , TE <sub>11,B</sub> TM <sub>01</sub>	TE <sub>11,A</sub> , TE <sub>11,B</sub> TE <sub>21,A</sub> , TE <sub>21,B</sub>	TE <sub>11,A</sub> , TE <sub>11,B</sub> TE <sub>21,A</sub> , TE <sub>21,B</sub>
Parasitic modes		TM <sub>01</sub> , TM <sub>11,A</sub> , TM <sub>11,B</sub>	TE <sub>01</sub> , TE <sub>31,A</sub> , TE <sub>31,B</sub> TE <sub>12,A</sub> , TE <sub>12,B</sub> TM <sub>01</sub> , TM <sub>11,A</sub> , TM <sub>11,B</sub> TM <sub>21,A</sub> , TM <sub>21,B</sub>

<sup>a)</sup>Electronic mail: thschang@phys.nthu.edu.tw.

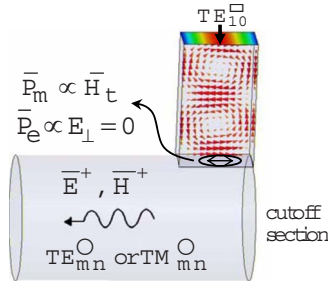


FIG. 1. (Color online) Coupling between a rectangular waveguide and a cylindrical waveguide.

( $e^{j\omega t}$ ),  $\mu_0$  is the permeability,  $\alpha_m$  is a constant that depends on the size and shape of the aperture, and  $H_z$  is the tangential magnetic field.

The resulting field in the cylindrical waveguide can be expressed as

$$\bar{E}^+ = \sum_n A_n^+ (\bar{e}_n + \hat{z}e_{zn}) \cdot e^{-j\beta_n z}, \quad (2a)$$

$$\bar{H}^+ = \sum_n A_n^+ (\bar{h}_n + \hat{z}h_{zn}) \cdot e^{-j\beta_n z}, \quad (2b)$$

where  $\bar{e}_n$ ,  $\bar{h}_n$ , and  $\hat{z}h_{zn}$  are the normalized field of the  $n$ th mode,  $A_n^+$  represents the amplitude of the  $n$ th mode, and  $h_{zn}(\phi) = (A \sin m\phi + B \cos m\phi) J_m(p'_{mn})$ . For a non-azimuthally symmetric mode (TE<sub>mn</sub> or TM<sub>mn</sub>,  $m \neq 0$ ), we can find two independent linearly polarized waves, denoted by the subindices  $A$  and  $B$ . The summation index  $n$  runs through all possible waveguide modes and + signs indicate forward propagating wave.

The amplitudes of the desired and the parasitic modes can be obtained by using the reciprocity theorem. The amplitudes of the two nonvanished modes are shown as follows:

$$A_{TE_{41},B}^+ = -\frac{4B}{P_{41}} \alpha_m H_{z0} j\omega \mu_0 J_4(p'_{41}), \quad (3a)$$

$$A_{TE_{01}}^+ = -\frac{4B}{P_{01}} \alpha_m H_{z0} j\omega \mu_0 J_0(p'_{01}) \neq 0, \quad (3b)$$

where  $P_n = 2\oint_{S_0} [(\bar{e}_n \times \bar{h}_n) \cdot \hat{z}] ds$  is a normalization constant proportional to the power flow of the  $n$ th mode. Other modal amplitudes equal zero. The power ratio of the major parasitic mode and the desired mode is

$$\frac{P_{01}^{\text{total}}}{P_{41}^{\text{total}}} = \frac{\beta_{41} p_{01}^4 \epsilon_{04} (p_{01}^2 - 0^2) J_0^4(p'_{01})}{\beta_{01} p_{41}^4 \epsilon_{00} (p_{41}^2 - 4^2) J_4^4(p'_{41})} = -18 \text{ dB}. \quad (4)$$

This means that the TE<sub>01</sub> mode will unavoidably be excited but fortunately, the other parasitic modes are completely suppressed. The working principle just presented provides the groundwork for estimating the mode purity, but it is unable to analyze the effect of frequency response. Therefore, a full wave solver, high frequency structure simulator (HFSS) is employed to simulate the real coupling structures.

**Mode purity analysis.** Figure 2 shows the simulated results of the mode purity. A rectangular waveguide mode is split into two or four equal and balanced input signals using the Y-type power divider (or cascade). The derived signals are then coupled to the cylindrical waveguide on the circumference. The arrangement of the couplings significantly re-

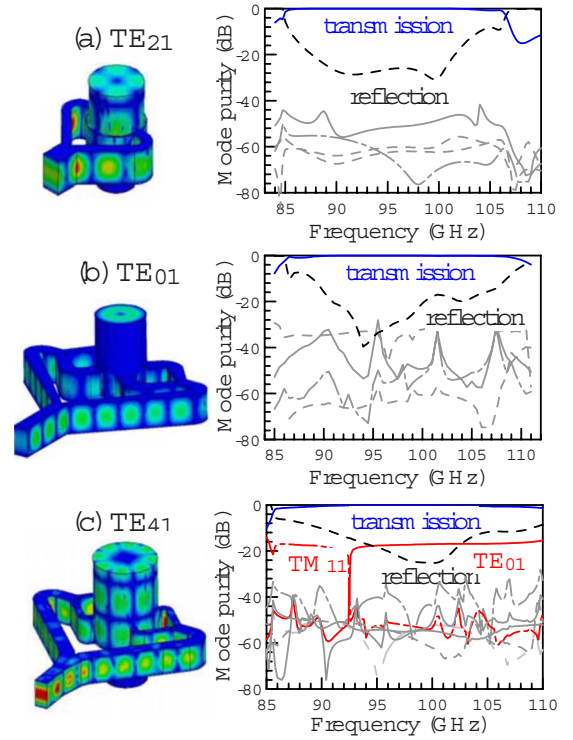


FIG. 2. (Color online) Simulated mode purity for a signal mode converter (a) TE<sub>21</sub>, (b) TE<sub>01</sub>, and (c) TE<sub>41</sub> modes. The simulated electric field patterns are also illustrated. The transmission and the reflection are shown as solid and dashed lines, respectively. The major parasitic modes are plotted in red and others are depicted in gray.

duces the excitation of the unwanted modes in the TE<sub>21</sub> and TE<sub>01</sub> mode converters. The HFSS simulation of a single mode converter verifies the theory. The concentrations of the spurious modes (gray lines) are basically less than  $-40$  dB as shown in Figs. 2(a) and 2(b). In addition, excitation of the TE<sub>41</sub> mode will unavoidably generate TE<sub>01</sub> mode (solid red line) as predicted in the theory. The simulation result, Fig. 2(c), agrees with the calculated one, i.e., Eq. (4). Notably, at low frequency region, the TM<sub>11</sub> mode (broken red line) replaces the TE<sub>01</sub> mode, but the concentration of the TE<sub>01</sub> and TM<sub>11</sub> modes is still low ( $-18$  dB) and acceptable for the gyrotron application.

**Experimental setup and measurement.** A back-to-back transmission method is commonly employed to characterize the performance of a mode converter for a broadband mea-

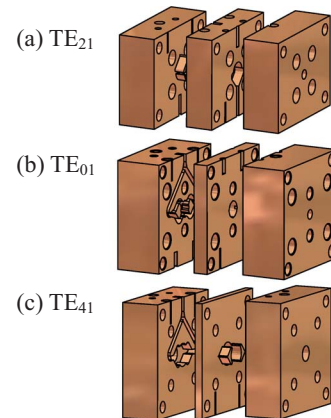


FIG. 3. (Color online) Design drawings for (a) TE<sub>21</sub>, (b) TE<sub>01</sub>, and (c) TE<sub>41</sub> modes.

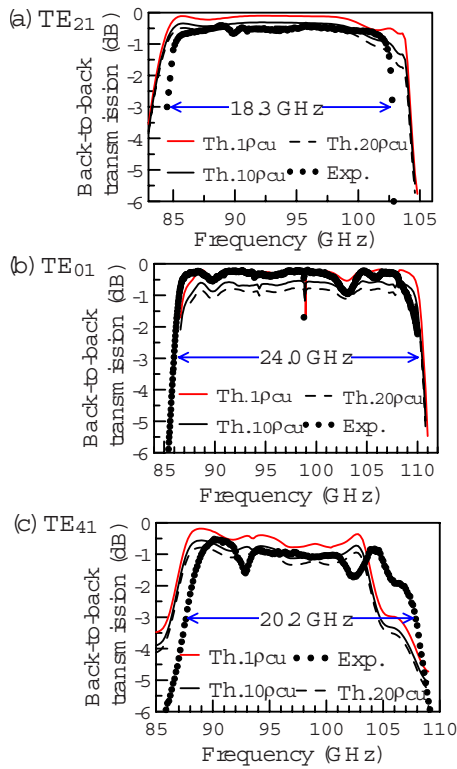


FIG. 4. (Color online) Frequency responses of the back-to-back transmissions for (a)  $TE_{21}$  mode, (b)  $TE_{01}$  mode, and (c)  $TE_{41}$  mode. The measured results are solid dots and the simulated results are lines. The effects of the wall resistivity are displayed.

surement. Figure 3 depicts the design drawings. Two identical converters are tightly joined with pins and screws. Each set consists of three pieces made of oxygen-free high-conductivity (OFHC) copper. The middle piece is a short uniform section of length around 3 mm. The plates are machined using a computer numerically controlled (CNC) lathe with a tolerance of  $5 \mu\text{m}$ . The ports are designed at opposite sides because the WR-10 flanges are too big to place at the same side. The transmission is measured with a well-calibrated two-port vector network analyzer (Agilent 8510C).

Figure 4 shows the HFSS simulations and experimental results for the back-to-back configuration. Generally speaking, the measured results are consistent with the HFSS simulation data. However, taking a closer look at Fig. 4 one will find that the measured values are slightly lower than the simulated ones even when considering the Ohmic loss of the OFHC copper. The dimensions of the W-band devices are generally small. Surface roughness due to machining might cause serious conductor loss. As a comparison, ten and twenty times of the resistivity of copper ( $\rho_{\text{cu}}$ ) are simulated

in addition to the standard value. The simulated and measured results, shown in Figs. 4(a) and 4(c), suggest that the appropriate resistivity is ten times of that of copper. However in Fig. 4(b) the experiment agrees very well with the theory ( $\rho = 1\rho_{\text{cu}}$ ). This might be due to the low conductor loss of the  $TE_{01}$  mode. It is worth to note here that the machining error is extremely critical in such high frequency devices. CNC machining is employed, but the yield rate is about 30%. Thus high-precision micromachining technique is preferred, such as LIGA (a German acronym for x-ray lithography, electroplating, and molding), if the devices are to be operated at the terahertz region.

The 3 dB transmission bandwidths are 18.3, 24.0, and 20.2 GHz for  $TE_{21}$ ,  $TE_{01}$ , and  $TE_{41}$  modes, respectively. They are the highest values ever reported to date. The proposed method has been demonstrated to be capable of exciting the desired mode with high converting efficiency, high mode purity, low reflection, and broad bandwidth. Such mode converters are suitable for a variety of applications at low terahertz region, especially the gyrotrons. For gyrotron applications, polarization controllability may be needed, which is not the focus of this paper (for more information, see Ref. 8).

This work was sponsored by the National Science Council, Taiwan. The authors are grateful to Professor S. J. Chung of National Chio Tung University for the measuring support and Mr. Charles Lee of Ansoft Corporation for the technical support.

<sup>1</sup>K. R. Chu, *Rev. Mod. Phys.* **76**, 489 (2004).

<sup>2</sup>W. Lawson, M. R. Arjona, B. P. Hogan, and R. L. Ives, *IEEE Trans. Microwave Theory Tech.* **48**, 809 (2000).

<sup>3</sup>D. B. McDermott, J. Petterebner, C. K. Chong, C. F. Kinney, M. M. Razeghi, and N. C. Luhmann, Jr., *IEEE Trans. Microwave Theory Tech.* **44**, 311 (1996).

<sup>4</sup>W. He, A. W. Cross, A. D. R. Phelps, K. Ronald, C. G. Whyte, S. V. Samsonov, V. L. Bratman, and G. G. Denisov, *Appl. Phys. Lett.* **89**, 091504 (2006).

<sup>5</sup>M. J. Buckley and R. J. Vernon, *IEEE Trans. Microwave Theory Tech.* **38**, 712 (1990).

<sup>6</sup>H. Guo, S. H. Chen, V. L. Granatstein, J. Rodgers, G. S. Nusinovich, M. T. Walter, J. Zhao, and W. Chen, *IEEE Trans. Plasma Sci.* **26**, 451 (1998).

<sup>7</sup>M. Blank, B. G. Danly, B. Levush, P. E. Latham, and D. E. Pershing, *Phys. Rev. Lett.* **79**, 4485 (1997).

<sup>8</sup>T. H. Chang and C. F. Yu, *Rev. Sci. Instrum.* **76**, 074703 (2005).

<sup>9</sup>C. F. Yu and T. H. Chang, *IEEE Trans. Microwave Theory Tech.* **53**, 3794 (2005).

<sup>10</sup>T. H. Chang, C. T. Fan, K. F. Pao, and K. R. Chu, *Appl. Phys. Lett.* **90**, 191501 (2007).

<sup>11</sup>A. H. McCurdy and J. J. Choi, *IEEE Trans. Microwave Theory Tech.* **47**, 164 (1999).

<sup>12</sup>K. C. Leou, D. B. McDermott, A. J. Balkcum, and N. C. Luhmann, Jr., *IEEE Trans. Plasma Sci.* **22**, 585 (1994).